COMMUNICATION

Check for updates

Synthesis of nanosized SAPO-34 with the assistance of bifunctional amine and seeds†

Pengfei Wu,[ab] Miao Yang,[a] Lijing Sun,[ab] Shu Zeng,[ab] Shutao Xu, [iD][a] Peng Tian*[a] and Zhongmin Liu [iD]*[a]

Nanosized SAPO-34 with a tunable silica content (acidity) has been synthesized with the assistance of bifunctional amine 1-[2-(2-hydroxyethoxy)ethyl]piperazine (HEEP) or its analog 1-(2-hydroxyethyl)-piperazine (HEP), in which the piperazinyl group acting as a co-template prompts the formation of the pure CHA phase, and the hydroxyl/ether groups help inhibit the crystal growth. The resultant nanocrystallines possess a large amount of Si(4Al) species, improve transport properties as confirmed by IGA, and thus exhibit enhanced MTO catalytic performance.

SAPO-34, as one of the most important representatives of the silicoaluminophosphate molecular sieve family, has attracted considerable attention due to its superior catalytic performance in the methanol-to-olefin (MTO) reaction.[1–3] The moderate acidity, special CHA structure with narrow 8-ring pore openings and large chabazite cages help the MTO reaction achieve 100% conversion and over 90% light olefin ($C_2^=$–$C_4^=$) selectivity. However, the diffusion limitation of the SAPO-34 catalyst is thus accentuated which leads to a fast coke deposition and a short catalytic lifetime. It is highly desirable to shorten the diffusion route, so that the coking rate can be retarded, and the catalytic lifetime can be prolonged while maintaining the high light olefin selectivity.

Previous reports have demonstrated various strategies such as the microwave assisted method, soft/hard template method, dry gel conversion method, etc. to decrease the crystal size or introduce mesoporous channels for SAPO-34.[4,5] Among them, effective methods for synthesizing SAPO-34 catalysts with good MTO catalytic performance are fewer, and in most cases the high synthesis cost and complicated procedure hinder their scale-up production. Amphiphilic organosilanes with long hydrophobic alkyl chains have been found to be effective mesoporogens to prepare hierarchical porous SAPO-34 with improved MTO catalytic performance.[6–8]

[a] National Engineering Laboratory for Methanol to Olefins, Dalian National Laboratory for Clean Energy, Dalian Institute of Chemical Physics, Chinese Academy of Sciences, Dalian 116023, China. E-mail: tianpeng@dicp.ac.cn, liuzm@dicp.ac.cn

[b] University of Chinese Academy of Sciences, Beijing 100049, P. R. China

However, it is still a big challenge to control the product silica content (acidity) in this system, because the mesoporogen is actually a part of the silica source during the crystallization. The organosilanes implanted into the SAPO-34 framework turn into silanol defects after calcination. As a result, ^{29}Si NMR reveals diverse Si environments, and the catalytic properties of hierarchical porous SAPO-34 cannot be arbitrarily judged through traditional experience. Given that the acidity is one of the important parameters determining the MTO catalytic performance of the catalyst besides mesoporosity, it is highly desirable to find silicon-free compounds for the synthesis of hierarchical/nanosized SAPO-34 catalysts.

In our previous works, a reconstruction method has been developed, which allows an easy control of the composition and porosity of the hierarchical SAPO-34.[6,9] The crystallization process is changed by the addition of sufficient ball-milled SAPO-34 precursor, which helps to go across the nucleation step and fasten the crystallization of mesoporous SAPO-34 single crystals. Another effort is to develop a new type of multifunctional organosilane. A short-chain organosilane 3-piperazinepropylmethyldimethoxysilane has been used as a "three in one" auxiliary to achieve SAPO-34 on the nanoscale.[10]
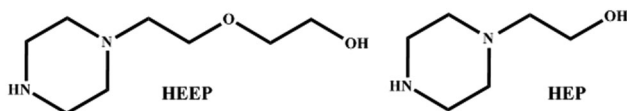
In this work, we provide commercial silicon-free compounds 1-[2-(2-hydroxyethoxy)ethyl]piperazine (HEEP) and 1-(2-hydroxyethyl)piperazine (HEP) for the synthesis of nanosized SAPO-34 with excellent MTO catalytic performance. HEEP/HEP contains simultaneously piperazinyl, hydrophilic hydroxyl and/or ether groups. The molecule structures of HEEP and HEP are shown in Scheme 1. It was reported that the molecules possessing abundant hydroxyl groups may cover the crystal nucleus surface, hinder their growth and obtain nanosized crystals.[11,12] Meanwhile the piperazinyl group has been proved by us to be efficient to direct the formation of the CHA framework.[10] Thus, HEEP and HEP are expected to be effective for the crystallization of nano SAPO-34 and allow the easy tuning of the product Si content.

HEEP/HEP-assisted synthesis of nanosized SAPO-34 was achieved with the use of a triethylamine (TEA) template and a small amount of ball-milled SAPO-34 seeds. The resultant products were designated as SP34-HEEP-s and SP34-HEP-s, respectively. To better understand the effect of HEEP/HEP,

Scheme 1 The molecular structures of the co-templates.

Fig. 1 XRD patterns of the as-synthesized samples. Asterisks indicate the AEI phase.

contrast syntheses were conducted by using piperazine (PIP) as a co-template instead of HEEP/HEP or without any co-template. The products were named as SP34-PIP-s and SP34-C-s. In parallel, syntheses without any seed were also done. The products were designated as SP34-HEEP, SP34-HEP, SP34-PIP and SP34-C, respectively. The initial SiO_2/Al_2O_3 molar ratio for all the samples was fixed at 0.31 in order to control the product Si content at a similar level. Their corresponding product phases and compositions are listed in Table 1.

The XRD patterns of the as-synthesized samples are displayed in Fig. 1. For the samples directed by TEA (SP34-C and SP34-C-s), peaks at 16.9 and 21.3 2θ degrees appeared (labeled with asterisks), suggesting the presence of the SAPO-34/18 intergrowth.[13,14] Upon the addition of PIP or its derivatives (HEEP and HEP), the SAPO-34/18 intergrowth phase was inhibited, which gave a typical CHA X-ray diffraction pattern. The results indicate that all three compounds containing piperazine groups facilitate the achievement of the pure CHA phase. This is important for the catalysts' MTO performance because the appearance of the intergrowth will decrease the selectivity to $C_2^=$ + $C_3^=$.[10] SEM images show the morphology of the products. The crystal sizes are quite different depending on the templates used. As seen in Fig. S1 (ESI†), the product presents rhombohedral crystals of about 5 μm in size when only TEA is used, and the crystals grow even bigger when PIP derivatives are added. Twinning crystals are the main products when HEEP or HEP was used together with TEA in comparison to the individual crystals obtained from the single TEA, and TEA plus PIP systems. When 5% seeds were introduced, the crystal size decreases sharply. Interestingly, the samples directed by TEA (Fig. 2a) and TEA + PIP (Fig. 2b) show uniform cubic morphology with particle sizes of about 1 μm, implying that the small molecule PIP has little effect on the product morphology. Surprisingly, SP34-HEEP-s (Fig. 2d) and SP34-HEP-s (Fig. 2c) presented approximately cubic morphology with a rough surface, and the primary particle sizes were about 150 and 400 nm, respectively. The particle size distributions of the samples were also
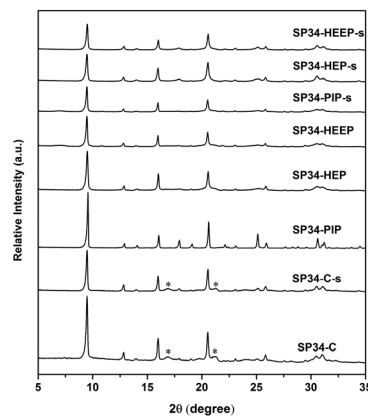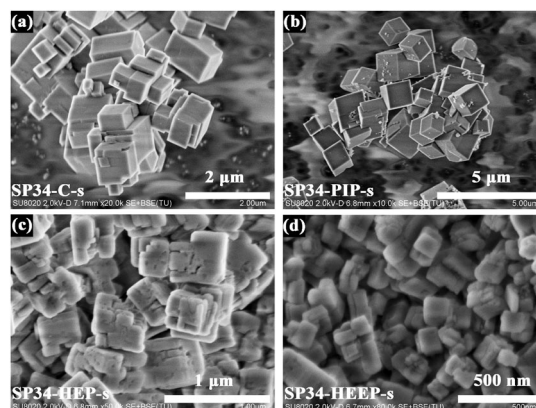

Fig. 2 SEM images of the calcined SP34-C-s (a), SP34-PIP-s (b), SP34-HEP-s (c), and SP34-HEEP-s (d).

measured by DLS (Fig. S2, ESI†), which give average particle sizes of 190 and 499 nm for SP34-HEEP-s and SP34-HEP-s, respectively. The above results suggest that the addition of HEEP and HEP can decrease the particle size heavily under the assistance of the seeds.

N_2 adsorption–desorption isotherms of SP34-HEEP-s and SP34-HEP-s are depicted in Fig. S3 (ESI†), and their textural properties are given in Table S1 (ESI†). Small hysteresis loops exist in the region $P/P_0 > 0.7$ for both samples, ascribed to the inter-crystal pores of nanoparticles. The samples SP34-HEEP-s and SP34-HEP-s exhibit increased external surface areas (35 m^2 g^{-1} and 33 m^2 g^{-1}) and higher mesopore volumes (0.12 cm^3 g^{-1} and 0.09 cm^3 g^{-1}) than those of micron-sized analogs. These characteristics would be beneficial for the diffusion of the product molecules so that the coking rate might be retarded during the MTO reaction.

Solid-state ^{29}Si and ^{13}C NMR spectra were collected to investigate the atomic chemical environments and the status of the template in the samples. The ^{29}Si MAS NMR spectra are shown in Fig. 3(a). The sharp signals centered at −92 ppm are attributed to the isolated $Si(OAl)_4$ environment. It has been conclusively shown that the $Si(OAl)_4$ species provide moderate acidic sites, which are beneficial for the MTO reaction.[3,15] The ^{13}C MAS NMR results are given in Fig. 3(b). Similar spectra are observed for SP34-C,

Table 1 Synthesis conditions, product composition and crystalline phase[a]

Sample	R	Seed (%)	Product composition	Crystalline phase
SP34-HEEP-s	HEEP	5	$Si_{0.089}Al_{0.485}P_{0.426}O_2$	SAPO-34
SP34-HEP-s	HEP	5	$Si_{0.086}Al_{0.520}P_{0.394}O_2$	SAPO-34
SP34-PIP-s	PIP	5	$Si_{0.085}Al_{0.470}P_{0.445}O_2$	SAPO-34
SP34-HEEP	HEEP	—	$Si_{0.084}Al_{0.486}P_{0.430}O_2$	SAPO-34
SP34-HEP	HEP	—	$Si_{0.084}Al_{0.487}P_{0.429}O_2$	SAPO-34
SP34-PIP	PIP	—	$Si_{0.084}Al_{0.475}P_{0.442}O_2$	SAPO-34
SP34-C-s[b]	—	5	$Si_{0.089}Al_{0.483}P_{0.428}O_2$	SAPO-34/18
SP34-C[b]	—	—	$Si_{0.086}Al_{0.484}P_{0.430}O_2$	SAPO-34/18

[a] The initial gel molar composition: $R/TEA/Al_2O_3/P_2O_5/TEOS/H_2O$ = 1.5/4.5/1.0/1.0/0.31/100 (200 °C, 24 h). [b] Pseudoboehmite used as an Al source and alkaline silica sol as a Si source. The initial gel molar composition: $TEA/Al_2O_3/P_2O_5/SiO_2/H_2O$ = 3.0/1.0/1.0/0.4/50 (200 °C, 24 h).

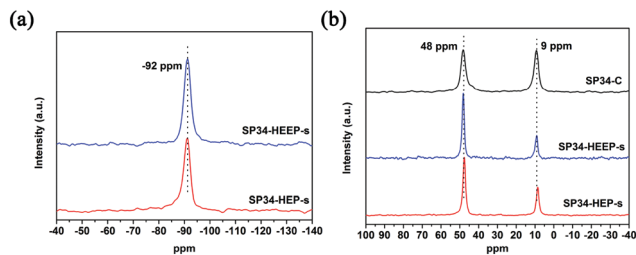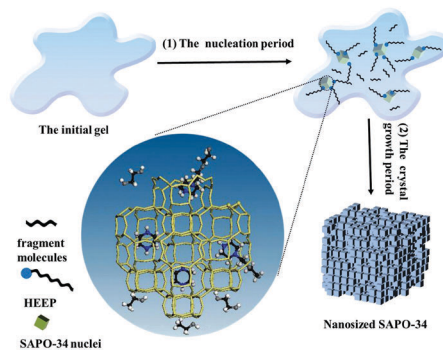**Table 2** Lifetime[a] and product distribution[b] of samples in the MTO reaction (WHSV = 2 h^{-1}, T = 450 °C), and calculated values of the inverse of the diffusion time constant (D/L^2)

Sample	Lifetime (min)	$C_2^=$ (%)	$C_3^=$ (%)	$C_2^= + C_3^=$ (%)	Coke content[c] (%, g g$_{cat}^{-1}$)	R_{coke}^c (mg min^{-1})	D/L^2 (s^{-1})
SP34-HEEP-s	446	50.83	33.62	84.45	27.81	0.062	8.36×10^{-2}
SP34-HEP-s	412	51.06	33.53	84.59	25.73	0.063	3.44×10^{-2}
SP34-PIP-s	242	51.26	34.01	85.27	19.05	0.079	—
SP34-C-s	327	48.01	33.73	81.75	23.89	0.073	—
SP34-C	208	43.25	37.17	80.42	20.65	0.099	1.15×10^{-3}
SP34-PZPMS[d]	376	50.00	33.65	83.65	25.19	0.064	1.08×10^{-1}

[a] Catalyst lifetime is defined as the reaction duration with >99% methanol conversion. [b] The highest selectivity of $C_2^=$ and $C_3^=$ under >99% methanol conversion. [c] Determined using a TG and DTA analyzer up to 800 °C measured after the MTO reaction. [d] From our previous work (ref. 10).

uptake curves of Fig. 4b, the propylene uptakes in the nanocrystals of SP34-HEEP-s and SP34-HEP-s are obviously much faster. It takes less than 9 min for the uptake to increase from 0 to 90%. Comparatively, the bulk SP34-C sample requires 372 min to achieve a similar uptake of 90%. Quantification of the diffusion properties was performed using Fick's second law (eqn (S1), ESI†).[17,18] Fig. S8 (ESI†) shows a linear relationship between $q(t)/q(\infty)$ and $t^{1/2}$, and the values of the inverse of the diffusion time constant (D/L^2) could be calculated from the slopes, which represent the mass transfer properties of the samples. As shown in Table 2, SP34-PZPMS has the largest D/L^2 value of 1.08×10^{-1}, while SP34-C has the minimum value of 1.15×10^{-3}. The D/L^2 values increase obviously with decreasing particle size of the samples, which implies that the gas phase product diffusion through the SP34-PZPMS, SP34-HEEP-s and SP34-HEP-s particles can be more effective than through SP34-C, which alleviates the formation of bulk coke species and facilitates the achievement of longer catalytic lifetimes. On the other hand, although SP34-PZPMS exhibits the shortest adsorption equilibrium time and the highest D/L^2 value, it exhibits a shorter catalytic lifetime and slightly worse light olefin selectivity than those of SP34-HEEP-s/SP34-HEP-s. We speculate that the result should be due to the difference in the acidity of the catalysts.

As seen from the NH$_3$-TPD results (Fig. S9, ESI†), SP34-PZPMS contains a smaller acid amount than SP34-HEEP-s and SP34-HEP-s, although their Si contents are comparable. The most likely cause of the decline in acid density for SP34-PZPMS is the introduction of organosilane, which generates Si–OH species in the calcined framework after the removal of organics. To confirm this speculation, solid-state ^{29}Si CP MAS NMR spectra were measured for the calcined SP34-PZPMS and SP34-HEEP-s. As shown in Fig. S10 (ESI†), the obvious shoulder peak at around −83 ppm of the calcined SP34-PZPMS could be attributed to the Si(OAl)$_n$(OH)$_{4-n}$ (n = 1 and 2) species.[19] These defect sites are useless (maybe harmful) for the MTO reaction.[20] Thus, it is concluded that the longer lifetime on SP34-HEEP-s and SP34-HEP-s than on SP34-PZPMS should result from the larger amount of single Si(4Al) environments, which provides more active sites with medium acidity for the reaction and contributes to the higher tolerance of the materials to the coke deposition.

In summary, by using the bifunctional amine HEEP/HEP together with a microporous template TEA, nanosized SAPO-34 was successfully synthesized. The pure CHA structure, good diffusion ability and large amount of Si(4Al) environment ensure that the catalyst exhibits an excellent MTO catalytic performance. In the future, more multifunctional amines are expected to be developed for the synthesis of hierarchical/nanosized SAPO catalysts with high efficiency.

Conflicts of interest

There are no conflicts to declare.

Notes and references

1 D. Chen, K. Moljord and A. Holmen, *Microporous Mesoporous Mater.*, 2012, **164**, 239–250.
2 M. Dusselier and M. E. Davis, *Chem. Rev.*, 2018, **118**, 5265–5329.
3 P. Tian, Y. Wei, M. Ye and Z. Liu, *ACS Catal.*, 2015, **5**, 1922–1938.
4 Q. Sun, Z. Xie and J. Yu, *Natl. Sci. Rev.*, 2017, **nwx103**, 1–17.
5 J. Zhong, J. Han, Y. Wei, P. Tian, X. Guo, C. Song and Z. Liu, *Catal. Sci. Technol.*, 2017, **7**, 4905–4923.
6 C. Wang, M. Yang, M. Li, S. Xu, Y. Yang, P. Tian and Z. Liu, *Chem. Commun.*, 2016, **52**, 6463–6466.
7 C. Wang, M. Yang, P. Tian, S. Xu, Y. Yang, D. Wang, Y. Yuan and Z. Liu, *J. Mater. Chem. A*, 2015, **3**, 5608–5616.
8 Q. Sun, N. Wang, D. Xi, M. Yang and J. Yu, *Chem. Commun.*, 2014, **50**, 6502–6505.
9 M. Yang, P. Tian, C. Wang, Y. Yuan, Y. Yang, S. Xu, Y. He and Z. Liu, *Chem. Commun.*, 2014, **50**, 1845–1847.
10 P. Wu, M. Yang, W. Zhang, S. Xu, P. Guo, P. Tian and Z. Liu, *Chem. Commun.*, 2017, **53**, 4985–4988.
11 D. Jin, Z. Liu, J. Zheng, W. Hua, J. Chen, K. Zhu and X. Zhou, *RSC Adv.*, 2016, **6**, 32523–32533.
12 C. Zhang, X. Lu and T. Wang, *J. Energy Chem.*, 2015, **24**, 401–406.
13 R. L. Smith, S. Svelle, P. del Campo, T. Fuglerud, B. Arstad, A. Lind, S. Chavan, M. P. Attfield, D. Akporiaye and M. W. Anderson, *Appl. Catal., A*, 2015, **505**, 1–7.
14 B. Gao, D. Fan, L. Sun, H. An, F. Fan, S. Xu, P. Tian and Z. Liu, *Microporous Mesoporous Mater.*, 2017, **248**, 204–213.
15 L. Xu, A. Du, Y. Wei, S. Meng, Y. He, Y. Wang, Z. Yu, X. Zhang and Z. Liu, *Chin. J. Catal.*, 2008, **29**, 727–732.
16 D. Wang, M. Yang, W. Zhang, D. Fan, P. Tian and Z. Liu, *CrystEngComm*, 2016, **18**, 1000–1008.
17 A. R. Teixeira, X. Qi, C.-C. Chang, W. Fan, W. C. Conner and P. J. Dauenhauer, *J. Phys. Chem. C*, 2014, **118**, 22166–22180.
18 D. Jin, G. Ye, J. Zheng, W. Yang, K. Zhu, M.-O. Coppens and X. Zhou, *ACS Catal.*, 2017, **7**, 5887–5902.
19 Z. Xue, J. Ma, W. Hao, X. Bai, Y. Kang, J. Liu and R. Li, *J. Mater. Chem.*, 2012, **22**, 2532–2538.
20 I. Yarulina, A. Dikhtiarenko, F. Kapteijn and J. Gascon, *Catal. Sci. Technol.*, 2017, **7**, 300–309.